

## Magnetic glass-ceramics

Viorel SANDU<sup>a,\*</sup>, Mirela Sidonia NICOLESCU<sup>a</sup>, Victor KUNCSE<sup>a</sup>,  
Raluca DAMIAN<sup>a</sup>, Elena SANDU<sup>b</sup>

<sup>a</sup> National Institute of Materials Physics, Magurele 077125, Romania

<sup>b</sup> "Horia Hulubei" National Institute of Nuclear Physics and Engineering, Magurele 077125, Romania

Received December 19, 2011; Accepted March 10, 2012

© The Author(s) 2012. This article is published with open access at Springerlink.com

**Abstract:** We present the magnetic properties of magnetic glass ceramics obtained by crystallization of Fe containing borosilicate glass. Two types of nucleators have been used: Cr<sub>2</sub>O<sub>3</sub> and P<sub>2</sub>O<sub>5</sub>. The role of the nucleators proved to be crucial in the size and morphology of the crystallites developed within glassy matrix as well in the magnetic response. The former stimulates the growth of regular single crystals uniformly dispersed within the matrix whereas the latter leads to the formation of grains made of tiny (30 nm), nanocrystals. The magnetic response depends on the amount of Fe ions left dispersed within glassy matrix as paramagnetic ions. Although P<sub>2</sub>O<sub>5</sub> leads to the best structural magnetite, almost 42% of Fe ions are left dispersed in the matrix without magnetic interaction. In the case of Cr<sub>2</sub>O<sub>3</sub>, the paramagnetic Fe is decreased to 12% but structural deficiency in the occupancy of the Fe sites of magnetite is revealed by Mössbauer spectroscopy.

**Key words:** glass ceramics; Fe<sub>3</sub>O<sub>4</sub>; Mössbauer spectroscopy; grain growth

### 1 Introduction

Magnetic glass ceramics constitute a special class of composite materials with magnetic nanocrystals embedded in a vitreous matrix. Although it has a composite character, this kind of ceramics is obtained from homogeneous glass melt through controlled crystallization of some magnetic constituents within the glassy matrix. The large compositional flexibility of the glass, which is based on the glass forming capability of a great number of compounds, opens the possibility to obtain new types and even classes of nanostructured materials by controlled crystallization.

The degree of freedom increases with increasing the number of glass constituents (polynar glass) and nucleators which allow a minute control of the ratio of different cations involved in the crystalline phase. For example, in a Fe ions containing glass melt, there are both Fe<sup>3+</sup> and Fe<sup>2+</sup> ions. The Fe<sup>3+</sup> ions enter tetrahedral coordination (FeO<sub>4</sub>) whereas Fe<sup>2+</sup> ions prefer octahedral coordination (FeO<sub>6</sub>). But Fe<sup>3+</sup> in tetrahedral coordination needs a charge compensation (e.g., from sodium) which might be also required by other trivalent metal like aluminum which also enter as AlO<sub>4</sub> in the glass network. Similarly, magnesium, which enters octahedral coordination with oxygen, competes in turn with Fe<sup>2+</sup>. Consequently, the quantity of Fe<sup>2+</sup> and Fe<sup>3+</sup> ions, hence, the nature of Fe-based phases which crystallizes within matrix, can be controlled by

\* Corresponding author.

E-mail: viorelsandu51@yahoo.com.

the interplay of the additional glass forming compounds.

That suppleness of glasses to form magnetic glass ceramics has led to a large diversity of nanostructured compounds with magnetic properties. By far, the most investigated system regards the Fe oxides, hematite and magnetite [1-8]. But many other magnetic compounds were obtained by crystallization within the glass matrix like  $\text{BaFe}_{12}\text{O}_{19}$  [9-16],  $\text{SrFe}_{12}\text{O}_{19}$  [17,18], Li-ferrite [16], Co-ferrite [19,20], Ni-Zn ferrites [21,22] and many others.

The interest for magnetic glass ceramics arises from the great potential for application which includes magnetic storage devices, MRI contrasting agents, magnetic hyperthermia, biodetection, microwave devices, waste sorbent, etc.

In the present contribution we communicate our results on the development of magnetite containing glass ceramic by crystallization of a Fe-rich borosilicate glass in the presence of small amount of  $\text{Cr}_2\text{O}_3$  or  $\text{P}_2\text{O}_5$  as nucleators.

## 2 Experimental

Two series of ferrimagnetic glass-ceramic composites were fabricated by crystallization of borosilicate glass melts with constant boron and sodium content (28.6 wt%  $\text{B}_2\text{O}_3$  and 6.4 wt%  $\text{Na}_2\text{O}$ ). The series have different content of iron oxide: one series contains 17.5 wt%  $\text{Fe}_2\text{O}_3$  whereas in the second the amount of  $\text{Fe}_2\text{O}_3$  is increased 24.5 wt%. Within each series, the samples differ by the nucleators used to trigger the process of crystallization: either 0.5 wt%  $\text{Cr}_2\text{O}_3$  or 1 wt%  $\text{P}_2\text{O}_5$ . Therefore, the samples with  $\text{Cr}_2\text{O}_3$  will be called  $\text{C}_i$ , whereas  $\text{P}_i$  will denominate the samples with  $\text{P}_2\text{O}_5$ , where  $i=1, 2$  stands for the series. Sample  $\text{C}_2$  contained also a certain amount of  $\text{Al}_2\text{O}_3$  (3.5 wt%). However, it is expected that all samples will incorporate a certain amount of aluminum since the melting process occurs in alumina crucibles.

The mixture of oxides ( $\text{SiO}_2$ ,  $\text{Fe}_2\text{O}_3$  and nucleators),  $\text{H}_3\text{BO}_3$  and,  $\text{Na}_2\text{CO}_3$  monohydrate, were melted in preheated alumina crucibles in contact with air and maintained for 2.5 hours at  $1470^\circ\text{C}$  except the sample  $\text{C}_1$  which was maintained 3 hours at  $1430^\circ\text{C}$ . The cast melts were further thermally treated at  $560^\circ\text{C}$  for two hours (six hours for the sample  $\text{C}_2$  due to the high content in alumina).

X-ray diffraction ( $\text{Cu K}_\alpha$  radiation, Bruker-AXS-

D8 Advance diffractometer), transmission electron microscopy (JEM 200CX TEM/SCAN), Mössbauer spectroscopy (constant acceleration spectrometer with a  $^{57}\text{Co(Rh)}$  radioactive and a proportional Xe gas counter) and magnetization (MPMS-Quantum Design) were used for the characterization of the samples.

The choice of nucleators was made in the attempt to investigate the effect of two different mechanisms for nucleation.  $\text{Cr}_2\text{O}_3$  acts through the strong field of the prevailing  $\text{Cr}^{6+}$  ions which has ordering effect on the oxygen ions and leads to the formation of spinel-type nuclei.  $\text{P}_2\text{O}_5$  promotes phase separation in borosilicate glass due to the charge difference between  $\text{Si}^{4+}$  and  $\text{P}^{5+}$ . The phosphorus-rich phase stabilizes the immiscibility of the two liquids and promotes the formation metal phosphate-rich regions as support for crystallization.

## 3 Results and discussions

The transmission electron microscopy (TEM) and Mössbauer spectroscopy were used as the most important tools for a correct characterization of the samples. In the analyze we start from the fact that in the cubic structure of the magnetite there are two sublattices, one which provides a tetrahedral coordination to the Fe ions (A site) and one within which Fe ions have a octahedral coordination (B site). In an ionic picture A sites are occupied by  $\text{Fe}_\text{A}^{3+}$  ions whereas the B sites are occupied equally and randomly by  $\text{Fe}_\text{B}^{3+}$  and  $\text{Fe}_\text{B}^{2+}$  ions at room temperature. Actually, at room temperature, there is a hopping of the electron between the two types of Fe ions in the octahedral positions which averages out the valence state to an intermediate value  $\text{Fe}^{+2.5}$ . For this reason, the ratio between the number of occupied in the octahedral and tetrahedral positions is  $R=2$  in the ideal magnetite. Any change of that value indicates the underoccupation of either tetrahedral positions ( $R>2$ ) or the octahedral positions ( $R<0$ ). Because the spin state of the Fe ion is  $S=5/2$  for  $\text{Fe}^{3+}$  and  $S=2$  for  $\text{Fe}^{2+}$ , in magnetically ordered state, the Mössbauer spectra must show two sextets corresponding to the splitting of the two types of ions. If the ions are in paramagnetic state, the spectra show only two doublets. The important aspect is that the ratio of the areas of the two sextets is proportional with the occupancy of the A and B sites.

Figure 1 presents the TEM micrograph of the

sample C<sub>1</sub>. It shows the presence of well separated nanocrystals uniformly embedded in the glassy matrix (Fig. 1). The electron diffraction pattern shows a unique phase which is magnetite. The deconvolution of the Mössbauer spectra (Fig. 2) gives  $R=2.1$  which indicates a small underoccupation of the tetrahedral sites. In the same time, the analysis of the doublets suggests that 16% of Fe is dispersed in the glassy matrix, with 10% of Fe<sup>3+</sup> in tetrahedral coordination.

The increase of Fe content leads to the formation of agglomerations of the nanoparticles of magnetite in grains larger than 250 nm. Each grain contains 10 to 15 nanocrystals of size of order 50 nm (Fig. 3). Although the magnetite nanocrystals are localized within grains, the latter are relatively uniformly distributed within sample.

Structurally, Mössbauer spectra shows that this time the octahedral positions are Fe-deficient with  $R=1.7$  (Fig. 4). It is interesting that this composition has the lowest level of iron dispersed in the paramagnetic state as Fe<sup>3+</sup>, only 12%. We attribute this low amount of Fe in the glassy matrix to the presence of Al<sup>3+</sup> ions, which competes with Fe<sup>3+</sup>.

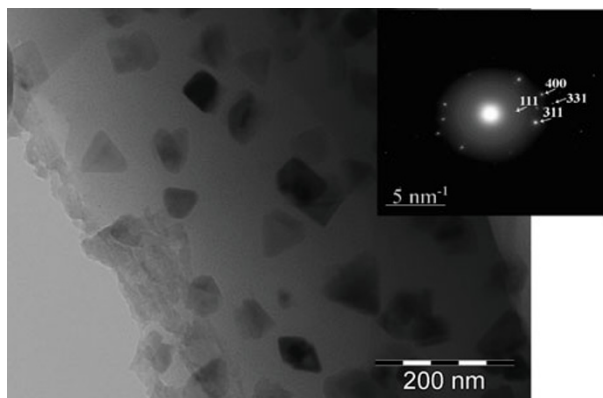


Fig. 1 TEM image and electron diffraction pattern of the sample C<sub>1</sub>

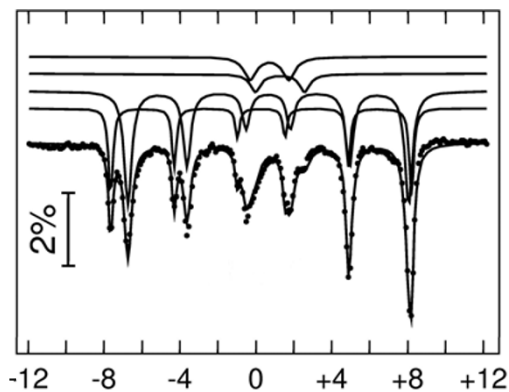


Fig. 2 Mössbauer spectra of the sample C<sub>1</sub>

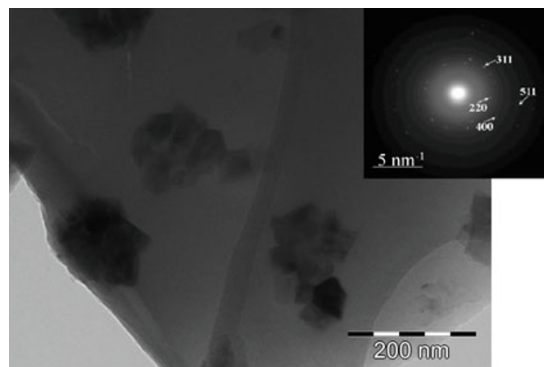


Fig. 3 TEM image and electron diffraction pattern of the sample C<sub>2</sub>

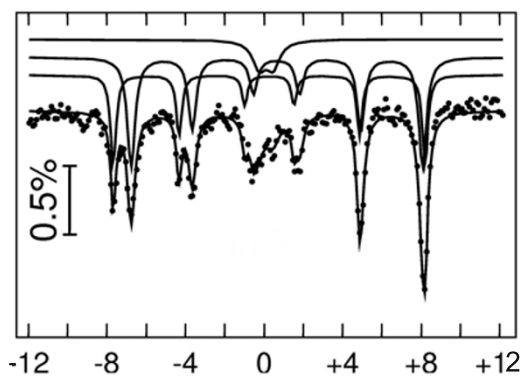


Fig. 4 Mössbauer spectra of the sample C<sub>2</sub>

P<sub>2</sub>O<sub>5</sub> generates agglomerations of tiny crystallites even at low Fe content. However, the grains are smaller and better packed because the size of the crystallites is smaller (Fig. 5). Mössbauer spectra (Fig. 6) are consistent with lower occupation of the octahedral sites since  $R=1.7$ . However, the amount of Fe in the crystalline state is much smaller, the huge doublets shows that 25% (22% in Fe<sup>3+</sup> state) of Fe is left as paramagnetic iron dispersed in the glassy matrix.

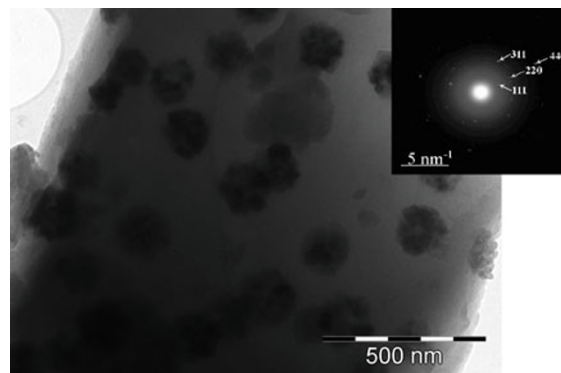
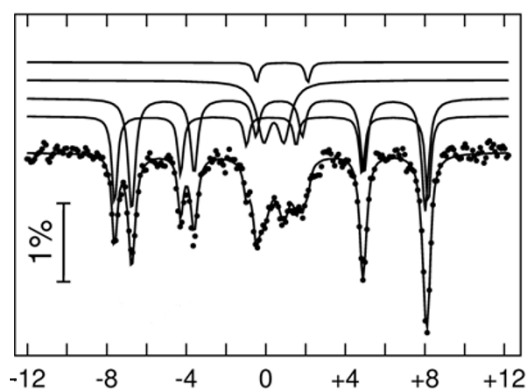
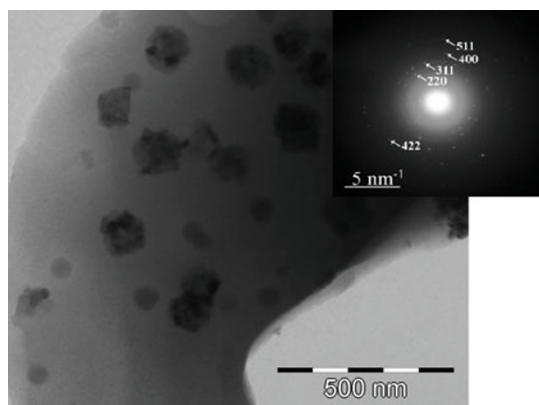
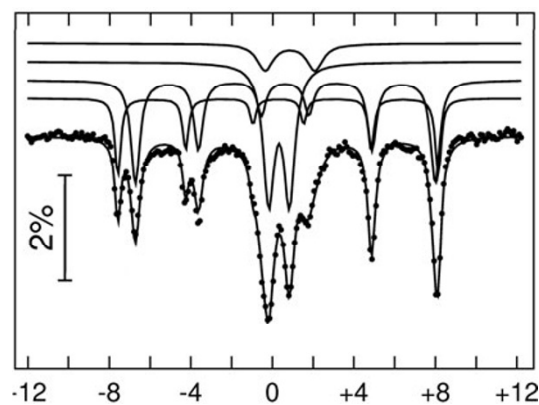


Fig. 5 TEM image and electron diffraction pattern of the sample P<sub>1</sub>

Fig. 6 Mössbauer spectra of the sample P<sub>1</sub>

The picture does not change too much when the amount of Fe is increased to 24.5 wt%. The nanocrystals become even smaller, smaller than 30 nm, but still build agglomerates whose shape gets more regular (Fig. 7). It is noteworthy that in this case we obtained the almost ideal magnetite with  $R=2$  as revealed by Mössbauer spectroscopy data (Fig. 8). However, 42% of iron was left dispersed within the glassy matrix in paramagnetic state.

Fig. 7 TEM image and electron diffraction pattern of the sample P<sub>2</sub>Fig. 8 Mössbauer spectra of the sample P<sub>2</sub>

In all cases only magnetite structure was revealed by electron diffraction. This state is confirmed by X-ray diffraction data (Fig. 9) where magnetite is almost the unique phase, except the sample C<sub>1</sub> where traces of  $\epsilon$ -Fe<sub>2</sub>O<sub>3</sub> are visible. The degree of crystallinity is higher in the samples obtained with Cr<sub>2</sub>O<sub>3</sub>: 52% in C<sub>1</sub> and 73% in C<sub>2</sub>. P<sub>2</sub>O<sub>5</sub> is less efficient in promoting crystallinity which remains below 50% in these samples (38.2% for P<sub>1</sub> and 45.1% for P<sub>2</sub>).

Ac magnetic susceptibility data shows different temperature dependence (Fig. 10a). The Verwey transition is obvious in all samples except the sample C<sub>1</sub> despite the fact that it has the largest crystals. However, a second transition, which is more visible in the imaginary part of the samples C<sub>1</sub>, C<sub>2</sub> and P<sub>1</sub>, is present at lower temperatures (Fig. 10b). This peak/shoulder below 35 K is present only in the samples with larger grain and might be related to the presence of the domain walls.

#### 4 Conclusions

Magnetic glass ceramic can be successfully prepared in a series of structures and shape using appropriate nucleators.

Cr<sub>2</sub>O<sub>3</sub> promotes the growth of large single crystal at low Fe content. However, some deficiency appears in the population of the two sublattices. Despite this effect this nucleator has the highest efficiency in promoting crystallization of the magnetite.

P<sub>2</sub>O<sub>5</sub> promotes small crystallites agglomerated in large almost spherical grains with a well defined Verwey transition, for any Fe content. At high Fe

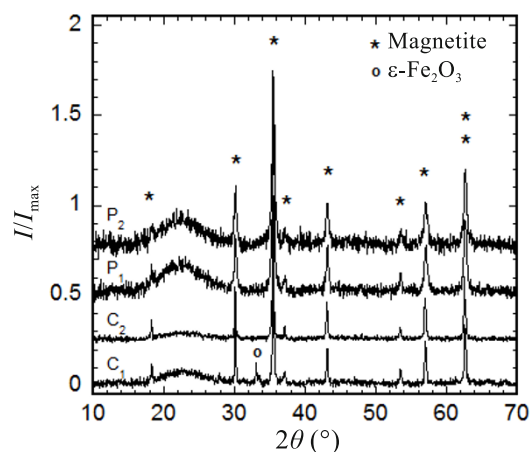


Fig. 9 X-ray diffraction patterns of the magnetite-based glass ceramic obtained by crystallization of Fe containing borosilicate glass melt.



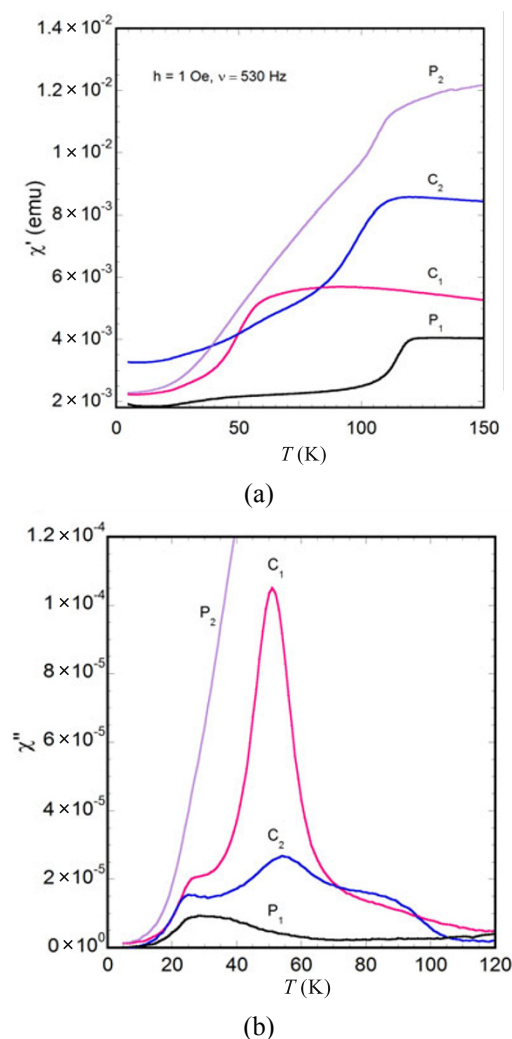


Fig. 10 *ac*-magnetic susceptibility of the magnetite-based glass ceramic obtained by crystallization of Fe containing borosilicate glass melt: (a) real part of the *ac*-susceptibility  $\chi'$ ; (b) imaginary part of the *ac*-susceptibility  $\chi''$ .

content, the magnetite is structurally perfect. However, an important amount of Fe ions, up to 42%, is left dispersed in the glassy matrix.

### Acknowledgments

This work was supported by the Romanian NASC under the Project EURATOM.

### References

[1] Hoell A, Kranold R, Lembke U, et al. Structural investigation of ferrimagnetic particles formed by glass crystallization. *Ber Bunsenges Phys Chem* 1996,

**100**: 1646-1650.

- [2] Tanaka K, Nakahara Y, Hirao K, et al. Preparation and magnetic properties of glass-ceramics containing magnetite microcrystals in calcium iron aluminoborate system. *J Magn Mag Mater* 1997, **168**: 203-212.
- [3] Mekki A, Ziq Kh A. Magnetic properties of a  $\text{SiO}_2\text{-Na}_2\text{O-Fe}_2\text{O}_3$  glass and glass ceramic. *J Magn Mag Mater* 1998, **189**: 207-13.
- [4] Kawashita M, Takaoka H, Kokubo T, et al. Preparation of magnetite-containing glass-ceramics in controlled atmosphere for hyperthermia of cancer. *J Ceram Soc Jpn* 2001, **109**: 39-44.
- [5] Woltz S, Hiergeist R, Görnert P, et al. Magnetite nanoparticles prepared by the glass crystallization method and their physical properties. *J Magn Mag Mater* 2006, **298**: 7-13.
- [6] Abdel-Hameed SAM, Hessian MM, Azooz MA. Preparation and characterization of some ferromagnetic glass-ceramics contains high quantity of magnetite. *Ceram Intern* 2009, **35**: 1539-1544.
- [7] Singh RK, Kothiyal GP, Srinivasan A. Magnetic and structural properties of  $\text{CaO-SiO}_2\text{-P}_2\text{O}_5\text{-Na}_2\text{O-Fe}_2\text{O}_3$  glass ceramics. *J Magn Mag Mater* 2008, **320**: 1352-1356.
- [8] Wisniewski W, Harizanova R, Völksch G, et al. Crystallisation of iron containing glass-ceramics and the transformation of hematite to magnetite. *Cryst Eng Commun* 2011, **13**: 4025-4031.
- [9] Oda K, Yoshio T, Oka K-O, et al. Morphology and magnetic properties of  $\text{BaFe}_{12}\text{O}_{19}$  particles prepared by the glass-ceramic method. *J Mater Sci Lett* 1985, **4**: 876-879.
- [10] Sohn S-B, Choi S-Y, Shim I-B. Preparation of Ba-ferrite containing glass-ceramics in  $\text{BaO-Fe}_2\text{O}_3\text{-SiO}_2$ . *J Magn Mag Mater* 2002, **239**: 533-536.
- [11] Rezlescu E, Rezlescu L, Popa PD, et al.  $\text{BaFe}_{12}\text{O}_{19}$  fine crystals dispersed in a glassy matrix: Magnetic and structural properties. *Mater Sci Eng: A* 2004, **375-377**: 1269-1272.
- [12] Chen GJ, Jian LY, Chang YS, et al. Preparation and properties of barium ferrite microcrystal in  $\text{B}_2\text{O}_3\text{-Bi}_2\text{O}_3$  glass. *J Cryst Growth* 2005, **277**: 457-461.
- [13] de Araújo JH, Cabral FAO, Ginani MF, et al. Synthesis and magnetic properties of the  $\text{SiO}_2\text{-BaFe}_{12}\text{O}_{19}$  glass-ceramic composites. *J Non-Cryst Solids* 2006, **352**: 3518-3521.
- [14] Müller R, Ulbrich C, Schüppel W, et al. Preparation and properties of barium-ferrite-containing glass ceramics. *J Eur Ceram Soc* 1999, **19**: 1547-1550.

- [15] Klupsch Th, Steinbeiss E, Müller R, et al. Magnetic glass ceramics- preparation and properties. *J Magn Mag Mater* 1999, **196-197**: 264-265.
- [16] Rezlescu N, Rezlescu L, Craus M L, et al.  $\text{LiFe}_5\text{O}_8$  and  $\text{BaFe}_{12}\text{O}_{19}$  fine particles crystallised in a glassy matrix. *Cryst Res Technol* 1999, **34**: 829-836.
- [17] Oda K, Yoshio T, Oka K-O. Magnetic properties of  $\text{SrFe}_{12}\text{O}_{19}$  particles prepared by the glass-ceramic method. *J Mater Sci Lett* 1984, **3**: 1007-1010.
- [18] Zaitsev DD, Kazin PE, Gravchikova EA, et al. Synthesis of magnetic glass ceramics containing fine  $\text{SrFe}_{12}\text{O}_{19}$  particles. *Mendelev Commun* 2004, **14**: 171-173.
- [19] Blackburn WJS, Tilley BP. The magnetic properties of glass-ceramics in the  $\text{CoO-Fe}_2\text{O}_3\text{-B}_2\text{O}_3$  system. *J Mater Sci* 1974, **9**: 1265-1269.
- [20] Chen W, Zhu M, Gao R, et al. Magnetic properties and microstructure of HDDR isotropic Nd-Dy-Fe-Co-B bonded magnets with high coercivity. *Sci China Ser A: Mathematics* 2002, **45**: 516-519.
- [21] Pal M, Brahma P, Chakravorty D, et al. Nanocrystalline nickel-zinc ferrite prepared by the glass-ceramic route. *J Magn Mag Mater* 1996, **164**: 256-260.
- [22] Singh RK, Srinivasan A. Magnetic properties of glass-ceramics containing nanocrystalline zinc-ferrite. *J Magn Mag Mater* 2011, **323**: 330-333.